Disruption of the *Arabidopsis* CGI-58 homologue produces Chanarin–Dorfman-like lipid droplet accumulation in plants

Christopher N. James[a,1], Patrick J. Horn[a,1], Charlene R. Case[a], Satinder K. Gidda[b], Daiyuan Zhang[a,c], Robert T. Mullen[b], John M. Dyer[c], Richard G. W. Anderson[d], and Kent D. Chapman[a,2]

[a]Department of Biological Sciences, Center for Plant Lipid Research, University of North Texas, Denton, TX 76203; [b]Department of Molecular and Cellular Biology, University of Guelph, Guelph, ON, Canada N1G 2W1; [c]United States Department of Agriculture-Agricultural Research Service, US Arid-Land Agricultural Research Center, Maricopa, AZ 85138; and [d]Department of Cell Biology, University of Texas Southwestern Medical Center, Dallas, TX 75390

Edited by Maarten J. Chrispeels, University of California San Diego, La Jolla, CA, and approved September 7, 2010 (received for review October 1, 2009)

***CGI-58* is the defective gene in the human neutral lipid storage disease called Chanarin-Dorfman syndrome. This disorder causes intracellular lipid droplets to accumulate in nonadipose tissues, such as skin and blood cells. Here, disruption of the homologous *CGI-58* gene in *Arabidopsis thaliana* resulted in the accumulation of neutral lipid droplets in mature leaves. Mass spectroscopy of isolated lipid droplets from *cgi-58* loss-of-function mutants showed they contain triacylglycerols with common leaf-specific fatty acids. Leaves of mature *cgi-58* plants exhibited a marked increase in absolute triacylglycerol levels, more than 10-fold higher than in wild-type plants. Lipid levels in the oil-storing seeds of *cgi-58* loss-of-function plants were unchanged, and unlike mutations in β-oxidation, the *cgi-58* seeds germinated and grew normally, requiring no rescue with sucrose. We conclude that the participation of *CGI-58* in neutral lipid homeostasis of nonfat-storing tissues is similar, although not identical, between plant and animal species. This unique insight may have implications for designing a new generation of technologies that enhance the neutral lipid content and composition of crop plants.**

compartmentation | plant lipid metabolism

Plants synthesize and store neutral lipids such as triacylglycerols (TAGs) primarily in cytosolic lipid droplets of maturing seeds (1, 2). In domesticated oilseeds, these stored TAGs represent a major source of calories for human and animal nutrition, an excellent feedstock for diesel fuels, and a reservoir for the deposition of industrially important fatty acids used as chemical feedstocks (3–6). Although not commonly appreciated, TAGs also are synthesized in nonseed tissues (7, 8), but their abundance in these tissues is low, in part because of the metabolism of the cell and perhaps as a consequence of the continuous recycling of fatty acids for energy and membrane synthesis. Indeed, vegetative cells can incorporate radiolabeled precursors into TAG (7, 8), they express diacylglycerol acyltransferases [the only enzyme in the "Kennedy pathway" unique to TAG production (9)], and they can accumulate TAGs in β-oxidation mutants (2) and in some floral (10) and fruit (7) tissues. Thus, although plant vegetative cells appear to have the metabolic machinery to synthesize and accumulate neutral lipids, there are likely underlying regulatory mechanisms in place to minimize this process, none of which are understood.

Chanarin-Dorfman syndrome is a neutral-lipid storage disease (11) caused by a defect in the protein CGI-58 (comparative gene identification-58, also called ABHD5 for α/β hydrolase-5). CGI-58 is a soluble enzyme that associates with cytosolic lipid droplets under certain metabolic conditions and appears to play a role in hydrolysis of stored lipids (11–14). Several different mutations in this protein, including amino acid substitutions, premature stop codons, and defects in mRNA splicing, have been identified in various Chanarin-Dorfman patients, all of which result in a hyperaccumulation of lipid droplets in tissues that do not normally store lipid (15). Thus, an understanding of the molecular mechanisms underlying this rare disease is important because it may provide new insights into how lipid homeostasis is regulated in nonfat-storing tissues (16). The precise mechanistic explanation for neutral lipid storage accumulation in Chanarin-Dorfman syndrome patients is uncertain, but the mammalian CGI-58 protein has been reported to be a coactivator of TAG lipases (12, 13, 15), thereby providing a connection between loss of CGI-58 activity and decreased TAG breakdown in *cgi-58*-defective cells. On the basis of the Chanarin-Dorfman phenotype, we hypothesized that a loss-of-function mutation in the *Arabidopsis CGI-58* homolog would lead to hyperaccumulation of lipid droplets in nonseed cells. Here we demonstrate that T-DNA disruption of the *CGI-58* locus in *Arabidopsis* does indeed result in accumulation of neutral lipids in mesophyll cells of leaves, and that these TAGs contain predominantly leaf-type fatty acid molecular species. These results indicate that CGI-58 is involved in neutral lipid homeostasis in plant cells and that, similar to its general function in mammalian cells, a loss-of-function mutation results in a significant increase in neutral lipids in nonlipid-storing cells.

Results

Searches of the *Arabidopsis thaliana* genome databases revealed a likely homolog to human *CGI-58* (Fig. 1*A*). The *Arabidopsis* gene locus, *At4g24160*, is expressed as two alternative transcripts: a longer full-length isoform (At4g24160.1) and a smaller isoform (At4g24160.2) missing a portion of the 3′ end (Fig. 1 *A* and *B*). Both mRNAs code for a protein that is homologous to the human CGI-58 protein and other orthologous members of this ABHD family (Fig. 1*A*). The long form of the *Arabidopsis* protein contains a conserved –HxxxxD– acyltransferase motif near its C terminus that is missing from the short form (Fig. 1*A*). Interestingly, the human CGI-58 protein has lysophosphatidic acid acyltransferase (LPAAT) activity but not lipase activity (17, 18). In contrast, the plant and yeast proteins possess a canonical lipase sequence motif [-GXSXG-, (Fig. 1*A*)] that is absent from vertebrate (humans, mice, and zebrafish) proteins. Although the plant and yeast CGI-58 proteins appear to possess detectable amounts of TAG lipase and phospholipase A activities in addition to LPAAT activity (19), the human protein does not (17, 20).

Author contributions: K.D.C. designed research; C.N.J., P.J.H., C.C.R., S.K.G., and D.Z. performed research; R.T.M., J.M.D., and R.G.W.A. analyzed data; and R.T.M., J.M.D., R.G.W.A., and K.D.C. wrote the paper.

The authors declare no conflict of interest.

This article is a PNAS Direct Submission.

Freely available online through the PNAS open access option.

[1]C.N.J. and P.J.H. contributed equally to this work.

[2]To whom correspondence should be addressed. E-mail: chapman@unt.edu.

This article contains supporting information online at www.pnas.org/lookup/suppl/doi:10.1073/pnas.0911359107/-/DCSupplemental.

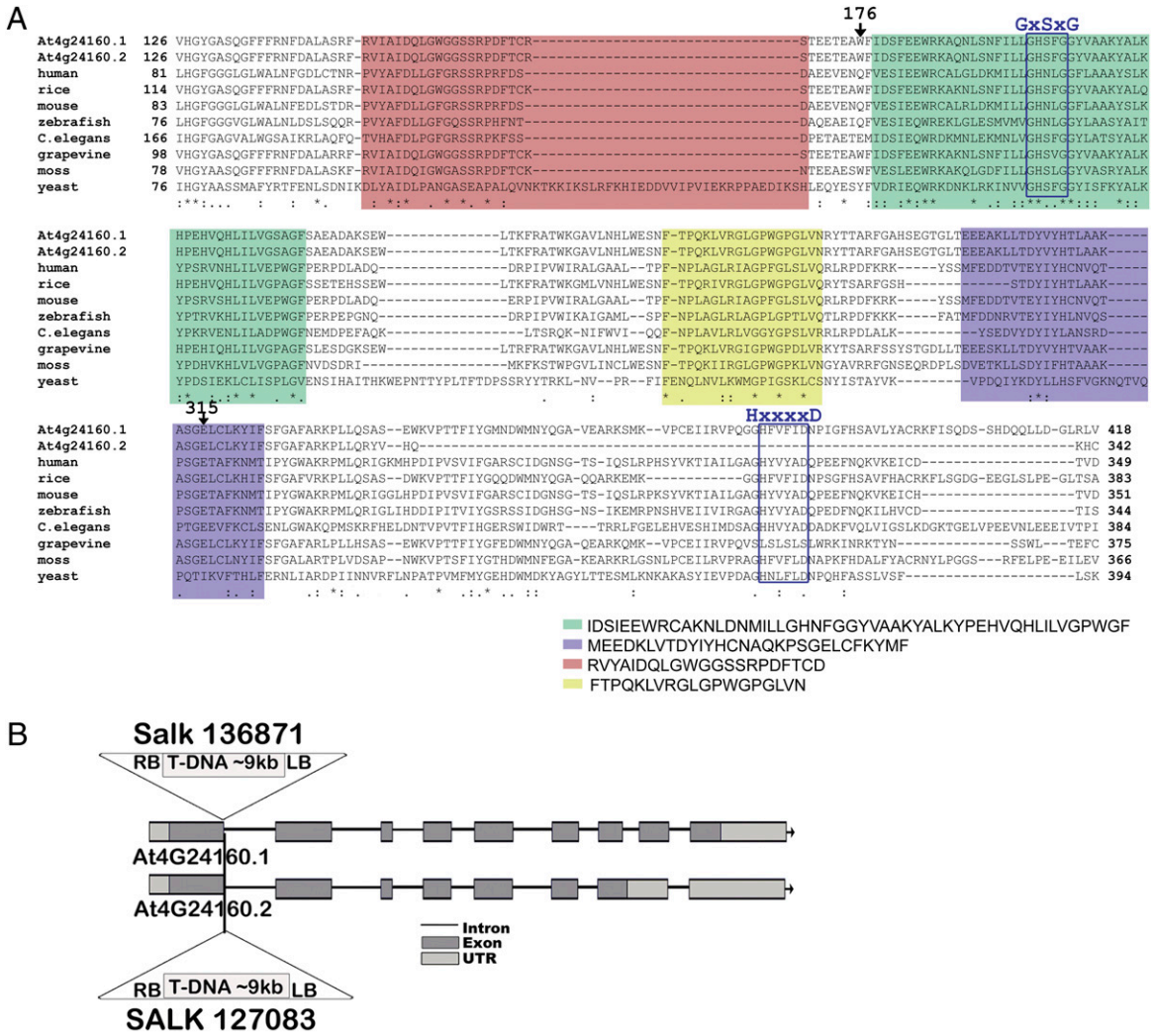

Fig. 1. Description of the *Arabidopsis CGI-58* homolog. (*A*) Partial amino acid sequence alignments of the *Arabidopsis* CGI-58 splice variants (At4g24160.1 and At4g24160.2) and homologs from grape, rice, human, mouse, *Caenorhabditis elegans*, zebrafish, moss (*Physcomitrella*), and yeast. Motif analysis by MEME/MAST (http://meme.sdsc.edu/meme4_4_0/intro.html) revealed three distinct domains common to all proteins (red, green, and blue). A fourth conserved region (yellow) was evident upon visual inspection. Two positions in the *Arabidopsis* protein marked 176 and 315 correspond to amino acid residues that, when mutated in the human sequence, interfere with lipid droplet-binding (and cause disease) (47). (*B*) The At4g24160 locus gives rise to two transcripts and the relative gene exon/intron/UTR structures are shown (redrawn based on information from www.arabidopsis.org). Two T-DNA insertional mutant lines were annotated in the SALK collection.

Two *Arabidopsis* lines with reported T-DNA disruptions in the first exon and intron of the *CGI-58* locus (SALK_136871 and SALK_127083, respectively; both sequenced and annotated by the J. Ecker laboratory, Salk Institute, La Jolla, CA) were identified (Fig. 1*B*). Compared with wild-type seedlings, both T-DNA mutant lines showed an abundance of lipid droplets in leaf tissues as visualized with the neutral-lipid-selective fluorescent dye, Nile red (Fig. 2 *A–C*, Fig. S1). The mutant plants also contained elevated neutral lipids rich in TAGs (Fig. 2*D*). In addition, considerably more lipid droplets were isolated from mutants compared with wild-type tissues (Fig. 2 *E–G*) by flotation through sucrose layers.

Approximately one-dozen individual, isolated lipid droplets were collected directly into a nanospray glass tip, microextracted with solvent, and analyzed by nanospray MS (Fig. 3). The major lipids in these droplets were indeed TAG, and tandem MS of TAG molecular ions verified the acyl assignments of the major TAG species (e.g., Fig. S2). The composition of TAG molecular species analyzed directly from lipid droplets was similar between wild-type and *cgi-58* mutants and also was similar to whole-leaf tissue TAGs (Fig. 3). Previously, ectopic overexpression of seed transcription factors was shown to increase TAG content in *Arabidopsis* seedling tissues, and this appeared to be caused by an up-regulation of a seed-specific program (21) because the TAG profiles were more similar to that in seeds; that is, the TAGs in the overexpression mutants were rich in the 20:1/eicosenoic fatty acid typically found in *Arabidopsis* seed oil bodies (2). Analysis of TAGs in aboveground vegetative tissues of *cgi-58* mutant plants by electrospray ionization (ESI) and tandem MS showed that their molecular composition was similar to that found in wild-type leaves (Fig. 3 and Fig. S2). That is, these TAGs were composed of typical leaf-tissue fatty acids such as 16:3/hexadecatrienoic and 18:3/octadecatrienoic fatty acids and did not contain 20:1 fatty acid (Fig. S2). Moreover, the TAG profiles in the *cgi-58* mutants were reminiscent of TAG composition generated in leaf tissues of *Arabidopsis* β-oxidation mutants (22, 23). Lipid droplet increase and distribution in leaves of *cgi-58* mutants were similar to that of the *acx1*/*acx2* double mutants that were blocked in β-oxidation (Fig. S3). However, unlike *acx1*/*acx2* double knockouts, seedlings of *cgi-58* mutants grew normally and did not require rescue on sucrose. Collectively, these results indicate that disruption of *CGI-58* in

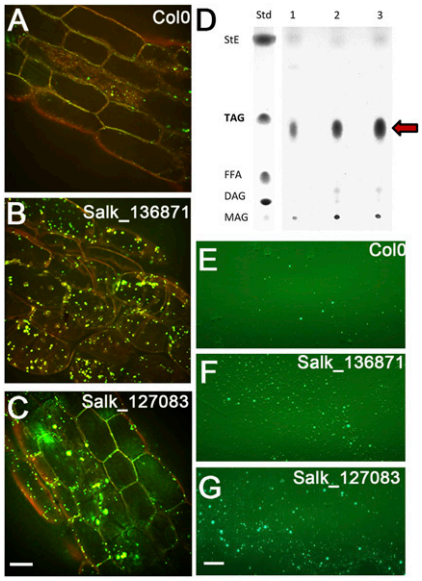

Fig. 2. Accumulation of lipid droplets in *Arabidopsis* plants that harbor a disruption in the *CGI-58* gene. Representative confocal fluorescence micrographs of (*A*) wild-type (Col 0) and two homozygous T-DNA mutant lines [SALK_136871 (*B*), and SALK_127083 (*C*)] stained with Nile red to reveal lipid droplets in 21-d-old seedlings (petiole region of true leaves). (Scale bar, 20 μm.) (*D*) TLC separation of the neutral lipid fraction isolated from liquid cultured 21-d-old seedlings (450 mg FW each) of wild-type (lane 1) and T-DNA mutants (lanes 2 and 3). Standards are steryl esters (StE), TAG (arrow), free fatty acids (FFA), diacylglycerols (DAG), and monoacylglycerols (MAG). (*E*–*G*) Representative epifluorescence micrographs of purified lipid droplets that were obtained from equivalent amounts of wild-type and mutant seedlings (stained with BODIPY 493/503). (Scale bar, 20 μm.)

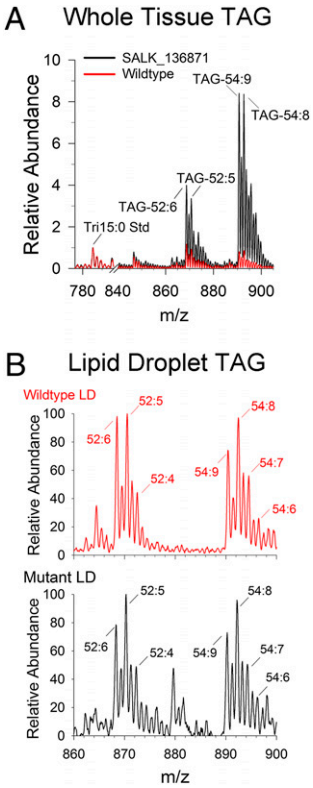

Fig. 3. MS analysis of TAGs in tissues and in isolated lipid droplets from leaves of wild-type (red) and *cgi-58* disrupted mutants (black). (*A*) Positive-ion MS analysis of neutral lipids extracted from leaves (overlay of representative spectra). TAG species are labeled according to the total acyl chain length followed by the number of double bonds present in each TAG molecular species. (*B*) Representative MS scans of direct organelle MS analysis of lipids in isolated droplets from wild-type and mutant leaves.

Arabidopsis leaves, like the situation in many animal tissues, causes a dramatic increase in cytosolic, TAG-containing lipid droplets in tissues that otherwise do not accumulate fat stores.

Additional imaging experiments with BODIPY493/503, which has improved spectral characteristics compared with Nile red (24), especially in chloroplast-containing tissues, confirmed that there were more lipid droplets throughout the mesophyll cells of mutant leaves compared with wild-type leaves (Fig. 4 *A* and *B*). Imaging both chloroplasts and lipid droplets together in the mutants showed a dramatic elaboration of lipid droplets in mutants compared with wild-type leaf cells (Fig. 4 *A* and *B*). Moreover, 3D reconstructions of multiple *z*-stacked confocal images of mutants specifically revealed that the lipid droplets accumulated in the cytosol and not inside chloroplasts (Fig. 4*C*), which is unlike the lipid-rich plastoglobuli that tend to accumulate in the chloroplast stroma of stressed or senescing tissues (25). Morphometric particle analysis comparing wild-type and mutant mesophyll tissues revealed a marked increase in average numbers of lipid droplets in mutant cells compared with wild-type cells, whereas the areas occupied by chloroplasts in these same groups of cells were approximately equivalent (Fig. 4*D*). Plots of frequency distribution of lipid droplets confirmed an increase in numbers of cells with increased numbers of lipid droplets in mutants compared with wild-type (Fig. 4*E*). Notably, there was a difference in cytosolic lipid droplet abundance depending upon the developmental stage of the leaves; that is, there were significantly more lipid droplets in mature, fully expanded leaves (e.g., 40-d-old) than either in younger leaves (15 d) or older, senescing leaves (65 d) of the mutants (Fig. S1).

Publicly available microarray analysis resources for *Arabidopsis* (e.g., Genevestigator; www.arabidopsis.org) showed that At4g24160 is constitutively expressed, but did not provide information about the relative expression of alternative transcripts. Using semiquantitative RT-PCR, we found that the longer (full-length) transcript was expressed in all wild-type tissues examined, whereas the shorter, truncated transcript was expressed, albeit at low levels, only in leaves and roots of wild-type (40 d) mature plants and in seedlings cultured in liquid or solid media (Fig. S4). The longer (full-length) transcript was also the major form detected in vegetative tissues of soil-grown, wild-type plants (Fig. S4). Neither transcript was detected in any tissues from mutants (Fig. S4), confirming the lack of *CGI-58* expression in these plants. Based on these results, it is likely that the larger CGI-58 protein product is responsible for regulating neutral lipid accumulation in vegetative tissues.

There were substantial changes in glycerolipid content and class composition in leaves of *cgi-58* mutants vs. wild-type plants. Overall, there was a significant increase in total fatty acid content on a dry-weight basis (Fig. 5*A*, *Inset*). The fatty acid composition of total leaf lipids was similar between *cgi-58* knockouts and wild-type, except for a small, but significant change in 16:0 and 18:3 content (Fig. 5*A*). Neutral lipids, specifically TAGs and steryl esters, showed the most relative change between mutants and wild-type (Fig. 5 *B* and *C*). The total amount of TAG in leaves of mature *Arabidopsis cgi-58* mutant plants, quantified by direct electrospray MS was more than 10-fold higher than in wild-type plants (Fig. 5*C*; see also representative spectra overlays in Fig. 3). The major glycerolipid membrane species were quantified by ESI-MS (26) and their amounts were summed and plotted as the relative change to wild-type levels (Fig. 5*C*, dotted line). Glycolipids and phospholipids were grouped for simplicity. The membrane acyl-lipids

PLANT BIOLOGY

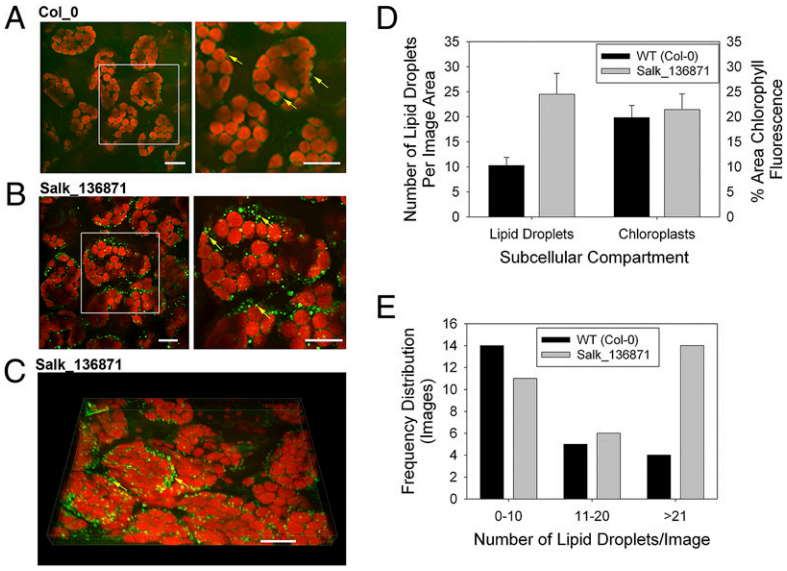

Fig. 4. Lipid droplets are abundant in leaves of *cgi-58* mutants. (*A*) Representative confocal fluorescence micrograph of mesophyll tissues of mature wild-type leaves, showing chloroplasts (red) and a few lipid droplets (arrows) stained with BODIPY 493/503 (green). (*B*) Confocal fluorescence micrograph of mesophyll tissues of same-age leaves of *cgi-58* T-DNA knockouts. (*C*) A *z*-stack of thirteen optical sections of the *cgi-58* T-DNA knockout mutant (Salk_136871). (*D*) Averages and SDs of lipid droplet numbers are plotted for 10 digital images of 25,000 μm^2, each taken from several leaves ($P < 0.005$). (*E*) The frequency of images with different numbers of lipid droplet numbers. (Scale bars, 20 μm.)

of chloroplasts (i.e., the glycolipids: MGDG, DGDG, SQDG, and PG) were increased in the *cgi-58* mutants, whereas most major phospholipids (PC, PE, PI, and PS) remained relatively unchanged (Fig. 5*C*). These results support the view that CGI-58 participates in the regulation of lipid turnover in vegetative cells, perhaps involving the recycling of fatty acids from plastidial membrane lipids, and that the disruption of this process causes abnormal amounts of TAG to accumulate in the cytosol. These observations are reminiscent of the *tgd4* mutants of *Arabidopsis*, which exhibit perturbed exchange of acyl lipids between chloroplasts and the endoplasmic reticulum and increases in TAG (27). Notably, seeds of *cgi-58* mutants showed no significant differences in amounts of storage lipid compared with wild-type (≈34% by weight in either wild-type or mutant seeds), indicating that CGI-58 likely does not play a role in TAG accumulation in seed tissues. Indeed, there were no delays or defects in seed germination or seedling establishment of the *cgi-58* T-DNA knockouts, suggesting that CGI-58 does not play a significant role in TAG mobilization during postgerminative growth.

Under certain metabolic conditions, the CGI-58 protein in humans reversibly associates with lipid droplets through its physical interaction with the lipid droplet-bound protein perilipin (11–13, 28). This association of CGI-58 with perilipin appears necessary for CGI-58 to function as a coactivator of lipolysis in human tissues (15). However, we did not find any obvious homologs to perilipin in the *Arabidopsis* genome. When we transiently expressed the longer form of *Arabidopsis* CGI-58 fused to the GFP at its N terminus in *Arabidopsis* leaf epidermal cells, the fusion protein colocalized with a coexpressed red fluorescent protein serving as the cytosolic marker (Fig. S5, *Upper*). A similar cytosolic location was observed for CGI-58 fused to GFP at its C terminus, and for the shorter CGI-58 isoform fused (at either its N or C terminus) to GFP. Consistent with these results, there was no obvious association of the longer CGI-58 isoform fused to red fluorescent protein at its N terminus with endogenous lipid droplets in leaf epidermal cells (Fig. S5, *Lower*).

Discussion

Overall, this study and others suggest some key commonalities in the regulation of neutral lipid accumulation and turnover in nonlipid-storing cell types in plants and animals. The similarity in phenotype because of loss-of-CGI-58 function in animals and plants—dysregulation of neutral lipid metabolism and storage—suggests that CGI-58 may be involved in an evolutionarily conserved process that is fundamentally important to cellular lipid homeostasis in eukaryotes. It is becoming increasingly apparent that the lipid droplets in cells play active roles in cellular processes, and are not just deposits for carbon storage (29). Evidence points to an interaction of lipid droplets with other subcellular compartments (30–34) and the appearance and disappearance of lipid droplets in cells may generally be used as a transient compartment for membrane trafficking or as metabolic reservoirs for membrane acyl groups (35, 36). Still others have suggested a possible role for lipid droplets in signal transduction (37).

The ontogeny of lipid droplets in fat-storing tissues (such as plant seeds or adipose tissue) appears to be fundamentally different from the more dynamic pool of TAGs produced in nonlipid-storing tissues. Here, despite a significant increase in lipid droplets in leaves of *cgi-58* mutant plants, there were no obvious changes in total lipid content of *Arabidopsis* seeds or problems with germination and seedling establishment. Our results, consistent with those in animal systems, support the concept that CGI-58 participates in aspects of neutral lipid metabolism and lipid droplet dynamics that are important for cellular lipid homeostasis, and this may be a process generally conserved in eukaryotes to provide for cellular acyl lipid needs independent of long-term energy storage.

The apparent lack of lipid droplet association for *Arabidopsis* CGI-58 further suggests that there also may be some differences between plant and animal cells in the underlying mechanisms of CGI-58 action. For example, TAG lipase activity, in addition to LPAAT and phospholipase A activities, was detected in the *Arabidopsis* CGI-58 recombinant protein expressed in *Escherichia coli*, but this is not the case for the human protein (20). Thus, the plant CGI-58 protein may be capable of participating in lipid turnover directly without requiring an additional TAG lipase on the lipid droplet surface. Regardless, a cytosolic location for *Arabidopsis* CGI-58 is consistent with its prospective role in regulating the accumulation of cytosolic lipid droplets.

From a practical point of view, there are currently few strategies available for engineering lipid molecules in above-ground biomass in plants. Although a more detailed understanding of the compartmentation of TAG in vegetative plant tissues is required, the overproduction of lipid droplets in nonseed tissues may be exploited as part of an overall strategy to maximize the recovery of renewable resources from agricultural products. Indeed, enhancing the proportion of lipid content in vegetative tissues increases the overall energy content of plants. This concept of enhancing energy content of biomass was put forward recently by Ohlrogge

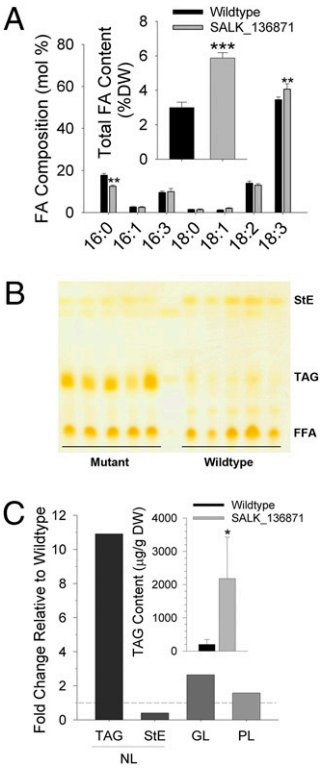

Fig. 5. Lipid composition analysis of *cgi-58* T-DNA knockout plants. (*A*) Total fatty acid composition and content (*Inset*) of leaves of 35-d-old plants. Means and SDs for five samples (**$P < 0.01$; ***$P < 0.000001$). (*B*) TLC separation of neutral lipid fractions collected from five replicate samples. Samples were spiked with heptadecanoic acid hence the appearance of substantial amounts of FFAs in all samples. (*C*) Fold-differences of *cgi-58*-derived lipid amounts compared with wild-type are plotted for neutral lipids (NL; includes both TAGs and StE); glycolipids (GL; includes monogalactosyldiacylglcerols, digalactosyldiacylglycerols, and sulfoquinovosyldiacylglycerols), and phospholipids (PL; includes phosphatidyl-choline, -ethanolamine, -inositol, glycerol, and phosphatidic acid) quantified by direct infusion ESI-MS (35). Values are averages summed from all major molecular species of polar and nonpolar lipids identified and then plotted as higher or lower relative to wild-type (dotted line). Quantities of TAG are plotted in the inset (*$P < 0.05$, $n = 5$).

et al. as a means of maximizing energy yield recovered after gasification (38). Alternatively, the elaboration of a neutral lipid compartment in leaves may facilitate an easy separation of the synthesis and compartmentation of unusual fatty acids for industrial purposes in a harvestable location outside the seed.

Materials and Methods

Plant Material. Two T-DNA insertional mutant lines were annotated in the SALK collection (39) and were obtained from the *Arabidopsis* stock center at Ohio State University. Seedlings were verified as homozygous for the T-DNA insert in the AtCGI-58 locus by PCR-typing, as directed by the SALK information site (http://signal.salk.edu/tdnaprimers.2.html). Plants grown in soil were maintained at about 21 °C in a 16-h/8-h light/dark cycle under grow lights at light levels between 45 and 65 $\mu E \cdot m^2 \cdot s$. Leaves were harvested at different stages for analysis. Alternatively, seeds were sown in half- strength Murashige and Skoog salts in liquid or solid medium with 1% sucrose (40) and seedlings were harvested at various intervals after sowing for analysis.

Imaging Lipid Droplets in Situ. Lipid droplets were imaged by confocal scanning fluorescence microscopy using either Nile red or BODIPY493 to selectively visualize lipid droplets in situ (24, 41). Tissues were fixed in 4% wt/vol paraformaldehyde in 50 mM Pipes pH 7.0 and stained with 6.5 mg/mL Nile red or 0.004 mg/mL BODIPY493/503. For Nile red imaging, excitation was at 495 nm and emission was at 568 and 624 nm. Images for Nile red fluorescence were obtained using the following parameters: gain, 16; 568, 3 s; and 624, 8 s. For BODIPY imaging, excitation of both chlorophyll and BODIPY were at 493 nm (imaging of chloroplasts and lipid bodies together). Emission wavelength for chlorophyll was 692 nm, exposed for 0.4 s. Emission wavelength for BODIPY-stained lipid droplets was 520 nm, exposed for 10 s, no gain. Images were acquired with a Zeiss 200M optical microscope fitted with a CSU-10 Yokogawa confocal scanner (McBain Instruments) and captured with a digital camera (Hamamatsu). Lipid droplet numbers and percent-area of chlorophyll autofluorescence were quantified using McMaster Biophotonics Facility (www.macbiophotonics.ca) and Image J software (National Institutes of Health, version 1.43T).

Lipid Body Isolation and Lipid Analysis. Lipid droplets were recovered by flotation centrifugation following the procedure of Liu et al. (42), and suspended in equal volumes of medium for staining, microscopic examination, and direct organelle MS. Lipid droplets were visualized on a glass slide under bright field and fluorescence microscopy. Approximately one-dozen droplets were collected in a glass nanospray tip (1-µm pore size; New Objective), microextracted into $CHCl_3$:MeOH in 10 mM ammonium acetate, and analyzed immediately by nanospray ionization mass spectrometry using an LCQ Deca XP Plus quadrupole ion trap.

Total lipids were extracted from plant tissues as described previously (43), except that tissues were homogenized with glass beads in hot isopropanol before monophasic extraction with $CHCl_3$ and water (44). Neutral lipids were fractionated from polar lipids by silica gel column chromatography in hexane:diethyl ether 4:1 by volume (Supelco Discovery DSC-Si 6 mL, 500-mg solid phase extraction cartridges), and separated by TLC in hexane:diethyl ether: acetic acid (80:20:1 by vol) on silica gel G plates (Whatman; visualized by acid-treatment and charring at 400 °F; 15 min; three times; or visualized by exposure to iodine vapor). Alternatively, lipid species including TAG were identified and quantified by direct-infusion, ESI-MS (35) as ammonium adducts $[M + NH_4]^+$ using a Waters Micromass Quattro Ultima triple quadrupole mass spectrometer (Waters). The neutral lipid fractions extracted from combined leaf tissues of mature plants (35-d-old, two plants per sample) were dissolved in 1:1 (vol/vol) chloroform:methanol with 10 mM ammonium acetate. TAG and steryl ester molecular species were identified by neutral loss fragmentation spectra in tandem (35) and quantified against tri-15:0 and cholesteryl ester (13:0), respectively. Detailed conditions are provided in *SI Materials and Methods*.

Polar lipids were identified by direct infusion ESI-MS (35) and quantities calculated based on a di-14:0 phosphatidylethanolamine internal standard. Glycolipid and phospholipid species were summed from quantitative results and presented as fold-difference between wild-type and mutant leaves. For total fatty acid analysis, a portion of each extract was transesterified in methanolic HCl and the purified methyl esters were quantified against a heptadecanoic acid internal standard by gas chromatography-flame ionization detector (26). Seed oil content was quantified by time-domain ^{1}H-NMR (45). All solvents were Optima grade from Thermo-Fisher Scientific.

RT-PCR. Transcript abundance was estimated by RT-PCR using a One-Step RT-PCR system from Takara Bio. The following transcript-specific primers were used for At4g24160 (F) 5′-ATGAACTTGAGCCGTTTTGCTTCGAGA-3′ (R1) 5′-AACCAATCGTAGACCATCTAGGAG-3′ (R2) 5′-GCAATGTTTTTGGTGGACATACCT-3′. Both long (R1) and short (R2) transcripts were amplified with the same forward primer but different reverse primers. RT-PCR reactions were performed with 0.2 µg total RNA and the following RT-PCR conditions: 42 °C for 15 min, and 95 °C for 2 min, followed by 35 cycles of 94 °C for 10 s, 56 °C for 25 s, 72 °C for 1 min 30 s. Amplification of ubiquitin transcripts was used as a control for comparisons. Amplimers were separated by agarose gel (1%) electrophoresis and visualized by ethidium bromide staining.

Transient Expression and Localization Assays. *Arabidopsis* CGI-58 proteins were expressed under control of the 35S promoter from the plasmid, pRTL2 (46), and images of cotransformed cells (via biolistic bombardment using a PDS-1000 system) (Bio-Rad Laboratories) were acquired using a Leica DM RBE microscope with a Leica 63× Plan Apochromat oil-immersion objective, a Leica TCS SP2 scanning head, and the Leica TCS NT software package (Version 2.61). Fluorophore emissions were collected sequentially; single-labeling experiments showed no detectable crossover at the settings used for data collection. Confocal images were acquired as a *z*-series of representative cells and single optical sections were saved as 512 × 512-pixel digital images.

ACKNOWLEDGMENTS. This research was supported in part by a grant from the Office of Science (Biological and Environmental Research), US Department of Energy Agreement DE-SC0000797, Natural Sciences and Engineering Research Council of Canada Grant 217291, US Department of Agriculture-Ag-

ricultural Research Service–Current Research Information System Project 5347-21000-009, the National Institutes of Health (HL-20948 and GM-52016), the Perot Family Foundation, and the Cecil H. Green Distinguished Chair in Cellular and Molecular Biology. (R.G.W.A.). We thank Dr. Lon Turnbull (University of North Texas) for advice and assistance with confocal microscopy. C.N.J. was supported by a Beth Baird Fellowship from the Department of Biological Sciences, and P.J.H. was supported by a Doctoral Fellowship from the Toulouse School of Graduate Studies (University of North Texas).

1. Tzen JT, Huang AH (1992) Surface structure and properties of plant seed oil bodies. *J Cell Biol* 117:327–335.
2. Graham IA (2008) Seed storage oil mobilization. *Annu Rev Plant Biol* 59:115–142.
3. Cahoon EB, et al. (2007) Engineering oilseeds for sustainable production of industrial and nutritional feedstocks: Solving bottlenecks in fatty acid flux. *Curr Opin Plant Biol* 10:236–244.
4. Damude HG, Kinney AJ (2008) Engineering oilseeds to produce nutritional fatty acids. *Physiol Plant* 132(1):1–10.
5. Dyer JM, Stymne S, Green AG, Carlsson AS (2008) High-value oils from plants. *Plant J* 54:640–655.
6. Napier JA (2007) The production of unusual fatty acids in transgenic plants. *Annu Rev Plant Biol* 58:295–319.
7. Murphy DJ (2001) The biogenesis and functions of lipid bodies in animals, plants and microorganisms. *Prog Lipid Res* 40:325–438.
8. Wu SS, et al. (1997) Isolation and characterization of neutral-lipid-containing organelles and globuli-filled plastids from *Brassica napus* tapetum. *Proc Natl Acad Sci USA* 94:12711–12716.
9. Dyer JM, Mullen RT (2008) Engineering plant oils as high-value industrial feedstocks for biorefining: The need for underpinning cell biology research. *Physiol Plant* 132(1): 11–22.
10. Lefèvre C, et al. (2001) Mutations in CGI-58, the gene encoding a new protein of the esterase/lipase/thioesterase subfamily, in Chanarin-Dorfman syndrome. *Am J Hum Genet* 69:1002–1012.
11. Lass A, et al. (2006) Adipose triglyceride lipase-mediated lipolysis of cellular fat stores is activated by CGI-58 and defective in Chanarin-Dorfman Syndrome. *Cell Metab* 3: 309–319.
12. Yamaguchi T, et al. (2007) CGI-58 facilitates lipolysis on lipid droplets but is not involved in the vesiculation of lipid droplets caused by hormonal stimulation. *J Lipid Res* 48:1078–1089.
13. Yamaguchi T, Omatsu N, Matsushita S, Osumi T (2004) CGI-58 interacts with perilipin and is localized to lipid droplets. Possible involvement of CGI-58 mislocalization in Chanarin-Dorfman syndrome. *J Biol Chem* 279:30490–30497.
14. Subramanian V, et al. (2004) Perilipin A mediates the reversible binding of CGI-58 to lipid droplets in 3T3-L1 adipocytes. *J Biol Chem* 279:42062–42071.
15. Yamaguchi T, Osumi T (2009) Chanarin-Dorfman syndrome: Deficiency in CGI-58, a lipid droplet-bound coactivator of lipase. *Biochim Biophys Acta* 1791:519–523.
16. Williams ML, Coleman RA, Placezk D, Grunfeld C (1991) Neutral lipid storage disease: A possible functional defect in phospholipid-linked triacylglycerol metabolism. *Biochim Biophys Acta* 1096(2):162–169.
17. Ghosh AK, Ramakrishnan G, Chandramohan C, Rajasekharan R (2008) CGI-58, the causative gene for Chanarin-Dorfman syndrome, mediates acylation of lysophosphatidic acid. *J Biol Chem* 283:24525–24533.
18. Ghosh AK, Ramakrishnan G, Rajasekharan R (2008) YLR099C (ICT1) encodes a soluble Acyl-CoA-dependent lysophosphatidic acid acyltransferase responsible for enhanced phospholipid synthesis on organic solvent stress in *Saccharomyces cerevisiae*. *J Biol Chem* 283:9768–9775.
19. Ghosh AK, Chauhan N, Rajakumari S, Daum G, Rajasekharan R (2009) At4g24160, a soluble acyl-coenzyme A-dependent lysophosphatidic acid acyltransferase. *Plant Physiol* 151:869–881.
20. Badeloe S, et al. (2008) Chanarin-Dorfman syndrome caused by a novel splice site mutation in ABHD5. *Br J Dermatol* 158:1378–1380.
21. Cernac A, Benning C (2004) WRINKLED1 encodes an AP2/EREB domain protein involved in the control of storage compound biosynthesis in *Arabidopsis*. *Plant J* 40: 575–585.
22. Yang Z, Ohlrogge JB (2009) Turnover of fatty acids during natural senescence of *Arabidopsis*, Brachypodium, and switchgrass and in *Arabidopsis* beta-oxidation mutants. *Plant Physiol* 150:1981–1989.
23. Slocombe SP, et al. (2009) Oil accumulation in leaves directed by modification of fatty acid breakdown and lipid synthesis pathways. *Plant Biotechnol J* 7:694–703.
24. Tavian D, Colombo R (2007) Improved cytochemical method for detecting Jordans' bodies in neutral lipid storage diseases. *J Clin Pathol* 60:956–958.
25. Munné-Bosch S (2005) The role of alpha-tocopherol in plant stress tolerance. *J Plant Physiol* 162:743–748.
26. Wanjie SW, Welti R, Moreau RA, Chapman KD (2005) Identification and quantification of glycerolipids in cotton fibers: Reconciliation with metabolic pathway predictions from DNA databases. *Lipids* 40:773–785.
27. Benning C (2009) Mechanisms of lipid transport involved in organelle biogenesis in plant cells. *Annu Rev Cell Dev Biol* 25:71–91.
28. Yamaguchi T, Omatsu N, Omukae A, Osumi T (2006) Analysis of interaction partners for perilipin and ADRP on lipid droplets. *Mol Cell Biochem* 284(1):167–173.
29. Goodman JM (2008) The gregarious lipid droplet. *J Biol Chem* 283:28005–28009.
30. Szymanski KM, et al. (2007) The lipodystrophy protein seipin is found at endoplasmic reticulum lipid droplet junctions and is important for droplet morphology. *Proc Natl Acad Sci USA* 104:20890–20895.
31. Liu P, Bartz R, Zehmer JK, Ying Y, Anderson RG (2008) Rab-regulated membrane traffic between adiposomes and multiple endomembrane systems. *Methods Enzymol* 439:327–337.
32. Fujimoto T, Ohsaki Y, Cheng J, Suzuki M, Shinohara Y (2008) Lipid droplets: A classic organelle with new outfits. *Histochem Cell Biol* 130:263–279.
33. Greenberg AS, Obin MS (2008) Many roads lead to the lipid droplet. *Cell Metab* 7: 472–473.
34. Olofsson SO, et al. (2008) Triglyceride containing lipid droplets and lipid droplet-associated proteins. *Curr Opin Lipidol* 19:441–447.
35. Bartz R, et al. (2007) Lipidomics reveals that adiposomes store ether lipids and mediate phospholipid traffic. *J Lipid Res* 48:837–847.
36. Zehmer JK, et al. (2009) A role for lipid droplets in inter-membrane lipid traffic. *Proteomics* 9:914–921.
37. Granneman JG, Moore HP (2008) Location, location: Protein trafficking and lipolysis in adipocytes. *Trends Endocrinol Metab* 19:3–9.
38. Ohlrogge J, et al. (2009) Energy. Driving on biomass. *Science* 324:1019–1020.
39. O'Malley RC, Alonso JM, Kim CJ, Leisse TJ, Ecker JR (2007) An adapter ligation-mediated PCR method for high-throughput mapping of T-DNA inserts in the *Arabidopsis* genome. *Nat Protoc* 2:2910–2917.
40. Teaster ND, et al. (2007) N-Acylethanolamine metabolism interacts with abscisic acid signaling in *Arabidopsis thaliana* seedlings. *Plant Cell* 19:2454–2469.
41. Greenspan P, Mayer EP, Fowler SD (1985) Nile red: A selective fluorescent stain for intracellular lipid droplets. *J Cell Biol* 100:965–973.
42. Liu P, et al. (2004) Chinese hamster ovary K2 cell lipid droplets appear to be metabolic organelles involved in membrane traffic. *J Biol Chem* 279:3787–3792.
43. Chapman KD, Moore TS, Jr (1993) N-acylphosphatidylethanolamine synthesis in plants: Occurrence, molecular composition, and phospholipid origin. *Arch Biochem Biophys* 301(1):21–33.
44. Bligh EG, Dyer WJ (1959) A rapid method of total lipid extraction and purification. *Can J Biochem Physiol* 37:911–917.
45. Todt H, Burk W, Schmalbein D, Kamlowski A (2006) Water/moisture and fat analysis by time-domain NMR. *Food Chem* 96:436–440.
46. Shockey JM, et al. (2006) Tung tree DGAT1 and DGAT2 have nonredundant functions in triacylglycerol biosynthesis and are localized to different subdomains of the endoplasmic reticulum. *Plant Cell* 18:2294–2313.
47. Schweiger M, Lass A, Zimmermann R, Eichmann TO, Zechner R (2009) Neutral lipid storage disease: genetic disorders caused by mutations in adipose triglyceride lipase/PNPLA2 or CGI-58/ABHD5. *Am J Physiol Endocrinol Metab* 297:E289–E296.

Supporting Information

James et al. 10.1073/pnas.0911359107

SI Materials and Methods

Lipid Droplet Isolation. Lipid droplets were recovered by flotation centrifugation following the procedure of Liu et al. (1), and suspended in equal volumes of medium for staining, microscopic examination, and MS. On this basis, lipid droplets isolated from mutant plants were more abundant than from wild-type. Routinely, equal fresh weights of plant tissues were homogenized and suspended in 20 mM Tricine-HCl (pH 7.8) and 250 mM sucrose. The suspension was then overlaid with 0.5 volume of 20 mM Pipes (pH 7.4), 100 mM KCl, and 2 mM $MgCl_2$ before centrifugation (60,000 × *g*, 90 min; Beckman 100Ti rotor, Beckman TL-100 centrifuge). The fat pad on the surface and residue around the wall of the tubes were collected and analyzed.

Direct Organelle MS Conditions. Approximately one-dozen lipid droplets, isolated from either mutant or wild-type leaves, were collected in a glass nanospray tip (1-μm pore size; New Objective), microextracted into $CHCl_3$:MeOH in 10 mM ammonium acetate, and analyzed immediately by nanospray ionization MS using an LCQ Deca XP Plus quadrupole ion trap. Triacylglycerol (TAG) molecular species were identified as their ammonium adducts $[M+NH_4]^+$. Typical scanning conditions were carried out in positive ion mode with a 0.8 to 1.2 kV spray voltage, scan range of 500 to 1,000 *m/z*, 200 °C capillary temperature, three microscans per full scan with a maximum injection time of 200 ms.

Direct Infusion Electrospray Ionization-MS (TAG Quantification). TAG and steryl ester molecular species from whole tissue extracts were identified by neutral loss fragmentation spectra in tandem (2) and quantified against tri-15:0 and cholestryl ester (13:0), respectively. Typical scanning conditions for a direct infusion rate of 12.5 μL/min were carried out in positive ion mode with a 3- to 3.5-kV spray voltage, 40-V cone voltage, and a scan range of 200 *m/z* to 1,050 *m/z*. The desolvation and source temperatures were maintained at 200 and 80 °C, respectively, and the desolvation and cone gas flows were set at 300 and 80 L/h, respectively. Tandem scans (MS/MS), whether detecting the precursor ions that lost a particular acyl chain in neutral-loss mode or single precursor-product species, were performed with collision energy of 30 V, with a scan range from 400 *m/z* to 1,050 *m/z*. Tripentadecanoyl glycerol (tri-15:0) was added at the time of extraction and used as a quantitative standard for TAG content (steryl esters were quantified against a cholesteryl decanoate standard and normalized to the tri-15:0 TAG standard).

1. Liu P, et al. (2004) Chinese hamster ovary K2 cell lipid droplets appear to be metabolic organelles involved in membrane traffic. *J Biol Chem* 279:3787–3792.

2. Bartz R, et al. (2007) Lipidomics reveals that adiposomes store ether lipids and mediate phospholipid traffic. *J Lipid Res* 48:837–847.

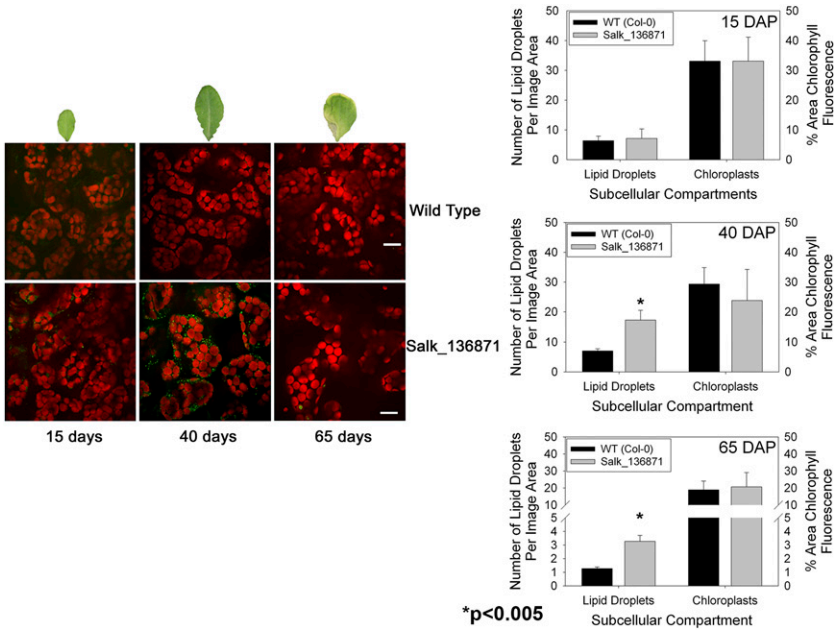

Fig. S1. Temporal differences in lipid droplet accumulation in wild-type and *cgi-58*-disrupted *Arabidopsis* plant cells. Representative confocal fluorescence micrographs of *Arabidopsis* leaves emerged at 15, 40, or 65 d (wild-type and T-DNA mutant, Salk_136871). Lipid droplets are green and chloroplasts are red; Imaging acquisition conditions were the same as for Fig. 4. The numbers of lipid droplets and the percent area of chloroplasts in mesophyll cells were quantified by morphometric analysis. Averages and SDs are plotted from 10 digital images of 25,000 μm^2, each over several leaves at each stage. There were significant differences (*$P < 0.005$) between the numbers of lipid droplets in mutants and wild-type leaves at 40 and at 65 d, but not at 15 d. Abundant droplets were most evident in mature fully expanded leaves of mutants. No statistical differences were observed in the relative percentage of chloroplasts between mutant and wild-type leaves. (Scale bars, 20 μm.)

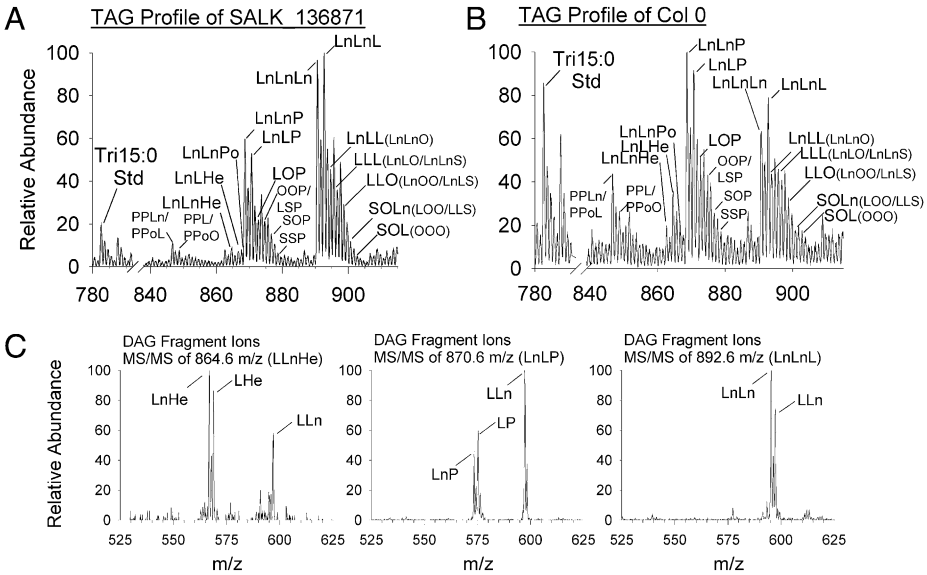

Fig. S2. Electrospray ionization MS of TAG molecular species in wild-type and *cgi-58* T-DNA knockout plants. Representative positive ion MS analysis of neutral lipids extracted from wild-type (*A*) and *cgi-58* (*B*) plants. TAG species are identified as ammonium adducts $[M + NH_4]^+$ and quantified against an added TAG standard (tri-15:0). Peaks are labeled according to the three fatty acids present in each TAG molecular species, and low abundance TAG species with the same molecular mass are indicated in parentheses. Positions of fatty acids on the glycerol backbone were not determined. Fatty acid abbreviations are: He, 16:3-hexadecatrienoic acid; L, 18:2-linoleic acid; Ln, α-18:3-linolenic acid; P, 16:0-palmitic acid; Po, 16:1-palmitoleic acid; S, 18:0-stearic acid. (*C*) Regions of several relevant, representative MS/MS scans showing the diagnostic diacylglycerol fragmentation ions minus a free fatty acid compared with known masses (1). Molecular ions were in some cases a combination of isomers as revealed in MS/MS (e.g., first two panels, each with three combinations of diacylglycerols (DAG) species derived from same parent ion, but with a different fatty acid loss).

1. Byrdwell WC (2005) The bottom-up solution to the triacylglycerol lipidome using atmospheric pressure chemical ionization mass spectrometry. *Lipids* 40:383–417.

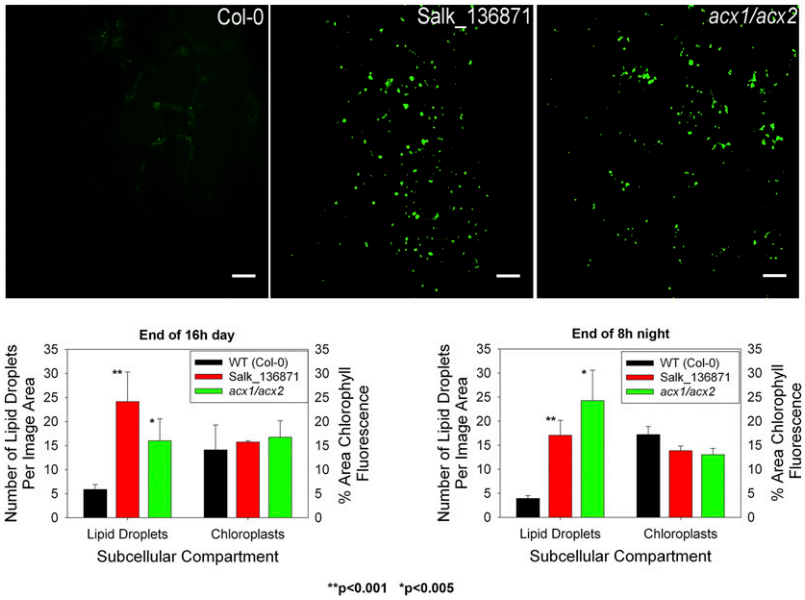

Fig. S3. Comparison of lipid droplet accumulation in *cgi-58* disrupted plants with acyl CoA oxidase double mutants (*acx1/acx2*), previously shown by Slocombe et al. (1) to accumulate lipid droplets in leaves. Representative confocal fluorescence micrographs of mature leaves of *Arabidopsis* WT (Col-0), the Salk_136871 mutant, and the *acx1/acx2* double knockout. Lipid droplets are green and imaging acquisition conditions were the same as for Fig. 4. Numbers of lipid droplets and the percent area of chloroplasts in mesophyll cells were quantified by morphometric analysis (*Lower*). Averages and SDs are plotted for 10 digital images of 25,000 μm^2, each taken from several leaves. There were significant differences between the amounts of lipid droplets in both mutants compared with wild-type leaves ($P < 0.005$) imaged at the end of a 16-h day and at the end of an 8-h night. No statistical differences were observed in the relative percentage of chloroplasts between mutants and wild-type. (Scale bar, 20 μm.)

1. Slocombe SP, et al. (2009) Oil accumulation in leaves directed by modification of fatty acid breakdown and lipid synthesis pathways. *Plant Biotechnol J* 7:694–703.

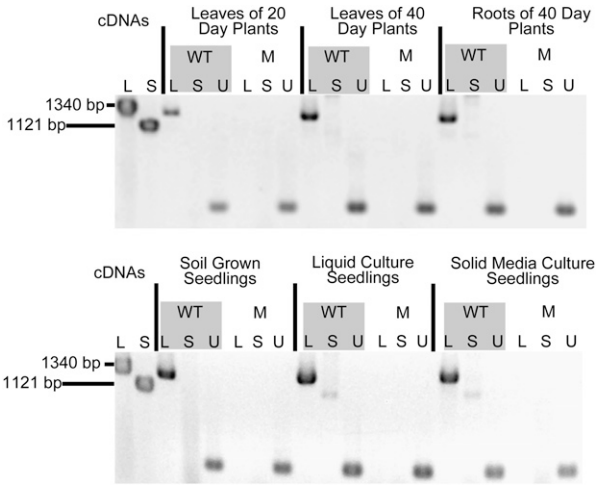

Fig. S4. Expression of At4g24160 (*CGI-58*) isoforms in different tissues and different developmental stages. Complementary DNAs corresponding to the two alternatively spliced At4g24160 (At4g24160.1 and At4g24160.2) transcripts (Fig. 1*B*) were amplified from seedling mRNA and used to verify sequences predicted in Fig. 1. Analysis of mRNA abundance using semiquantitative RT-PCR revealed that the longer splice variant (1,340 bp; lanes labeled "L" in each sample) was expressed in both leaves and roots of wild-type plants cultivated under a variety of conditions. The shorter splice variant (1,121 bp; lanes labeled "S"), however, was only detected at very low levels in leaves of 40-d-old plants, and seedlings grown on liquid or solid media. Notably, no transcripts for either the longer or shorter form of At4g24160 were detected in the T-DNA mutant plants (M). The level of ubiquitin transcripts expressed in the same wild-type and mutant plants (lanes labeled "U") are shown as a control.

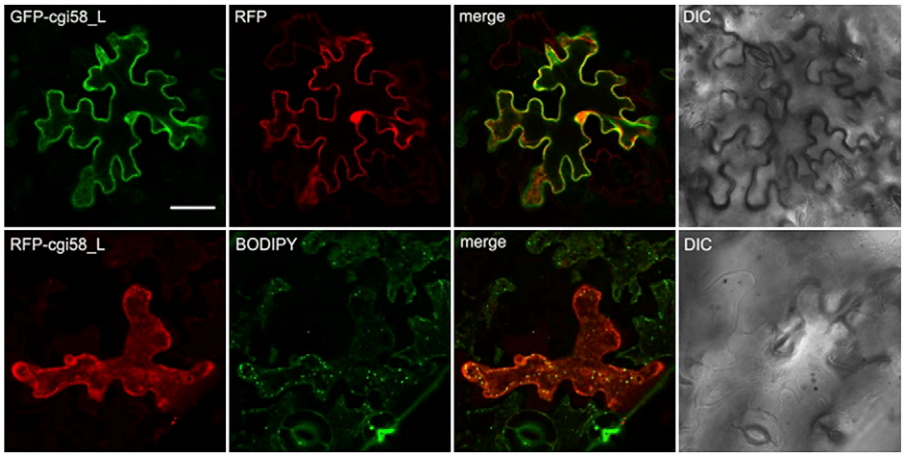

Fig. S5. CGI-58 localizes to the cytosol in *Arabidopsis* leaves. In transient expression studies, a GFP-CGI-58 fusion protein (consisting of GFP fused to the N terminus of the longer isoform of CGI-58; GFP-cgi58_L) was transiently coexpressed (via biolistic bombardment) with the red fluorescent protein (RFP) in epidermal cells of 25 d-old *Arabidopsis* leaves (*Upper*). The merged image of the two fluorophores indicates colocalization in the cytosol. The image to the right is of the same leaf cells acquired by differential interference contrast (DIC) microscopy. In a similar experiment, transiently expressed RFP-cgi-58_L localizes to the cytosol, and not to endogenous lipid droplets (stained with BODIPY). (Scale bar, 20 μm.)